

Fig. 6. Dependence of phase shift on half slit width  $L$  ( $A = 0.35$ ,  $G = 0.05$ ,  $B/D = 1.43$ ).

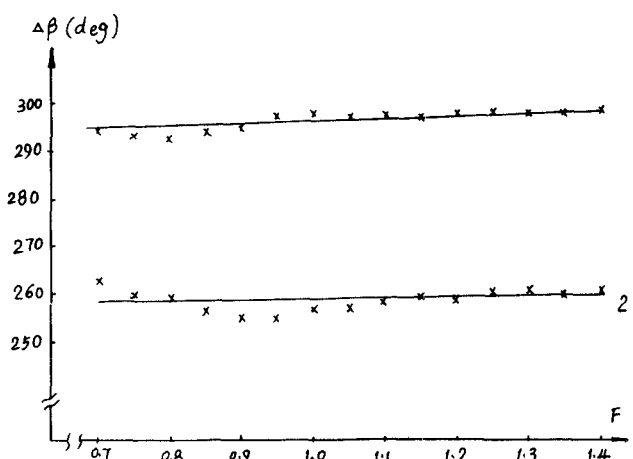


Fig. 7. Experimental phase shift characteristic of model using grooved waveguide (curve 1,  $A = 0.34$ ,  $G = 0.055$ ,  $B/D = 1.46$ ) and rectangular waveguide (curve 2,  $A = 0.316$ ,  $G = 0.05$ ).

#### IV. EXPERIMENTAL RESULTS

We have carried out experiments on toroidal phase shifter using both grooved and rectangular waveguide. By properly choosing the dimensions of toroid and waveguide, both of them may be made very broad band—more than one octave bandwidth. The phase shift versus frequency characteristics of these two models are shown in Fig. 7. The loss factor is approximately 0.8–1.0 dB/360°.

#### V. DISCUSSION

From the above theoretical and experimental results we may conclude that by properly choosing the dimensions, toroid phase shifters using grooved waveguides with reduced sizes possess many advantages—miniaturization, low loss, and wide bandwidth. Their loss factor is 16 percent lower than the models using rectangular waveguides. Therefore, they will find widespread applications in many practical uses.

#### ACKNOWLEDGMENT

The author thanks G. Zhang and J. Liu for their help in performing this study.

#### REFERENCES

- W. J. Ince, "Recent advances in diode and ferrite phaser technology for phased-array radars," *Microwave J.*, pp. 36–46, Sept. 1972.
- W. W. Siekanowicz, W. A. Schilling, T. E. Walsh, L. Bardash, and I. Gordon, "Design and performance of a 20-kilowatt latching nonreciprocal  $X$ -band phase shifter," *RCA Rev.*, vol. 26, no. 4, pp. 574–589, Dec. 1965.
- W. J. Ince and E. Stern, "Nonreciprocal remanence phase shifters in rectangular waveguide," *IEEE Trans. Microwave Theory Tech.*, vol. MTT-15, pp. 87–95, Feb. 1967.
- W. P. Clark, "A technique for improving the figure-of-merit of a twin-slab nonreciprocal ferrite phase shifter," *IEEE Trans. Microwave Theory Tech.*, vol. MTT-16, pp. 974–975, Nov. 1968.
- L. R. Whicker and R. R. Jones, "Design considerations for digital latching ferrite phase shifters," *Microwaves*, vol. 5, no. 11, pp. 31–39, Nov. 1966.
- G. P. Rodrigue, J. L. Allen, L. J. Lavedan, and D. R. Taft, "Operating dynamics and performance limitations of ferrite digital phase shifters," *IEEE Trans. Microwave Theory Tech.*, vol. MTT-15, pp. 709–713, Dec. 1967.
- R. A. Moore, G. M. Kern, and L. R. Cooper, "High average power S-band digital phase shifter," *IEEE Trans. Microwave Theory Tech.*, vol. MTT-22, pp. 626–634, June 1974.
- W. Hauth, "Accurate analysis of latching phase shifters," *Proc. Inst. Elec. Eng.*, vol. 133, pt. H, pp. 165–168, June 1986.
- A. Mizobuchi and H. Kurebayashi, "Nonreciprocal remanence ferrite phase shifters using the grooved waveguide," *IEEE Trans. Microwave Theory Tech.*, vol. MTT-26, pp. 1012–1016, Dec. 1978.
- Wen Junding, "Experimental studies of latching ferrite phase shifters of back-ridged waveguide," *Acta Electronica Sinica*, no. 3, pp. 44–51, Sept 1979.

#### Network Analyzer Calibration Using Offset Shorts

G. J. SCALZI, MEMBER, IEEE, A. J. SLOBODNIK, JR., MEMBER, IEEE, AND G. A. ROBERTS

**Abstract**—Microwave network analyzer accuracy enhancement by offset shorts is investigated. Usable calibration bandwidth and accuracy limitations are determined by applying a previously published model to the case of a reference short and two offset shorts. Data necessary to emulate the HP 8510 are derived and used in the model to provide realistic projections. A technique is presented for precise characterization of offset short standards.

#### I. INTRODUCTION

In order to minimize the systematic errors present during automatic network analyzer operation, accuracy enhancement or calibration procedures are normally followed [1]. The most common standards used to perform a one-port calibration consist of a short, an open, and a matched load [2], [3]. These broadband standards are readily available with coaxial connectors and are clearly preferred whenever the device under test (DUT) is also coaxial. However, with the increasing need to generate data for the design of monolithic microwave integrated circuits (MMIC's), chip-level devices must be measured in a microstrip environment. This causes problems for short, open, load calibration. A quality microstrip matched load and an accurately characterized microstrip open are not as easily achievable as a good microstrip short. One technique that can be used to overcome this difficulty and still permit accuracy enhancement to be performed right up to

Manuscript received April 1, 1987; revised December 21, 1987.

The authors are with the Electromagnetics Directorate, Rome Air Development Center, Hanscom AFB, MA 01731.

IEEE Log Number 8820447

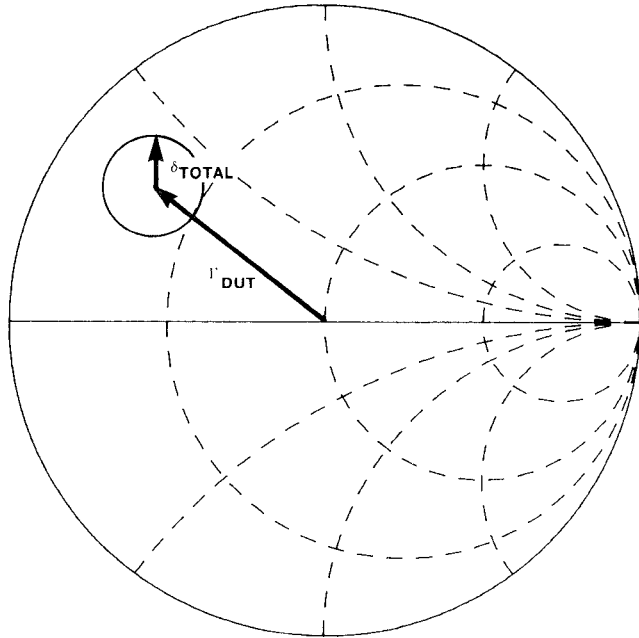


Fig. 1 Illustration of the definition of  $\delta_{\text{TOTAL}}$ .  $\Gamma_{\text{DUT}}$  may terminate anywhere within the uncertainty circle

the edge of the chip under test is the substitution of offset shorts for the open and the load [4], [5].

The purpose of this paper is to provide quantitative information on the bandwidth and accuracy limitations of this method and thus to delineate the range of validity of short, offset shorts calibration. These results will be generated by applying a previously published theory [6] to the use of offset shorts. Experimental results illustrating the use of the theory to optimize measurement accuracy and to characterize an offset short will also be presented.

## II. OUTLINE OF THE THEORY

The theory of Glasser [6] is used for the current study since it accurately models the operation of a network analyzer, that is, calibration with a particular set of standards and determination of the reflection coefficient,  $\Gamma$ , of a DUT. Errors in the knowledge of the standards as well as measurement errors are included. These input quantities are specified as radii of uncertainty circles,  $\delta_{2L}(\text{STD } i)$  and  $\delta_{1M}$ , in the reflection coefficients of the standards and measurements, respectively. Final output of the theory consists of a computed error circle radius,  $\delta_{\text{TOTAL}}$ , which is uncertainty in the reflection coefficient of the DUT. An example is shown in Fig. 1.

At this point it is useful to review some of the mathematics in a slightly generalized form. Begin by combining and expanding equations (10) and (15) of Glasser [6] in order to obtain an expression for the maximum value of the desired quantity:

$$\delta_{\text{TOTAL}} = \delta_{2M}(\text{DUT}) + \sum_{i=1}^3 [\delta_{2L}(\text{STD } i) + \delta_{2M}(\text{STD } i)] \cdot |h_{1i} + \Gamma_{\text{DUT}} h_{2i} + \Gamma_{\text{DUT}}^2 h_{3i}|. \quad (1)$$

Here

$$\begin{bmatrix} h_{11} & h_{12} & h_{13} \\ h_{21} & h_{22} & h_{23} \\ h_{31} & h_{32} & h_{33} \end{bmatrix} = \begin{bmatrix} 1 & \Gamma_{\text{STD}1} & \Gamma_{\text{STD}1}^2 \\ 1 & \Gamma_{\text{STD}2} & \Gamma_{\text{STD}2}^2 \\ 1 & \Gamma_{\text{STD}3} & \Gamma_{\text{STD}3}^2 \end{bmatrix}^{-1} \quad (2)$$

and

$$\delta_{2M}(\text{LOAD}) = \left| \frac{(1 - \Gamma_{\text{LOAD}} E_{22})^2}{E_{12} E_{21}} \right| \delta_{1M}. \quad (3)$$

$E_{jk}$  are the usual network analyzer error terms [7], and here a load represents either a standard or the DUT.

In order that the model reflect realistic conditions, a measurement error corresponding to the Hewlett-Packard 8510 network analyzer [8] was determined and used. This quantity was obtained as follows. Short, open, load standards with reported uncertainty [9] values of  $\delta_{2L}(\text{SHORT}) = 0.0$ ,  $\delta_{2L}(\text{OPEN}) = 0.0135$ , and  $\delta_{2L}(\text{LOAD}) = 0.003$  were input into the model, and  $\delta_{1M}$  (the other input parameter) was varied until  $\delta_{\text{TOTAL}}$  showed best agreement with the published HP 8510 total uncertainty [9], [10]. This procedure resulted in a value of  $\delta_M = 0.001$  for  $\Gamma_{\text{DUT}} = 0.0^\circ$ . Actual HP 8510 average error terms were also used in the model.

## III. COMPUTER RESULTS

A comparison of total error versus frequency for both short, open, load and short, offset shorts calibration is shown in Fig. 2. The former assumes a 7 mm coaxial system while the latter assumes a 0.5766-mm-wide microstrip on a 0.635-mm-thick alumina substrate. These microstrip conditions hold throughout this paper. Clearly the offset shorts technique is band limited. At low frequencies, offset short lengths become a small fraction of a wavelength and all these standards reduce to shorts. The next spike occurs when the longer offset short (STD3) rotates around the Smith Chart to again become degenerate with the short (STD1). For the third spike, all three standards are degenerate since here  $D_{\text{STD}3} = 2D_{\text{STD}2}$ . In general, spikes occur whenever

$$\not\Gamma_{\text{STD}i} - \not\Gamma_{\text{STD}k} = \pm n\pi \quad (n \text{ even}, i \neq k). \quad (4)$$

For  $k=1$  (which corresponds to a short) and  $i=2, 3$  (offset shorts),

$$2\beta D = \frac{4\pi f \sqrt{\epsilon_{\text{eff}}} D}{c} = n\pi \quad (5)$$

which can be readily solved for  $f$ . Here  $D$  is the offset length,  $\epsilon_{\text{eff}}$  is the relative effective dielectric constant [11], and  $c$  is the velocity of light.

Returning to Fig. 2, a bandwidth can be defined at the  $\delta_{\text{TOTAL}} = 0.015$  points. This is approximately twice the maximum error of the HP 8510 [9], [10]. Confining our attention to the first band, the computed bandwidth becomes 6.87 GHz at a center frequency of 5.29 GHz. However, both are functions of the magnitude and phase of the DUT. If anything other than a narrow range of DUT magnitude and phase is to be measured, then the total usable bandwidth shrinks considerably. It must be computed from the maximum lower band edge and minimum upper band edge over all DUT values. This usable bandwidth is illustrated in Fig. 3 and is plotted as a function of offset short length in Fig. 4. Here each curve represents a given value of uncertainty in the standards. For example,  $\delta_{2L} = 0.015$  corresponds to an angular uncertainty in the reflection coefficient of the standards of  $0.86^\circ$ . The curves of Fig. 4 cover  $|\Gamma_{\text{DUT}}| = 0.1$ , 0.5, and 0.9 for all DUT angles in  $10^\circ$  increments.

Fig. 4 can be used to determine an appropriate offset short length. For example, with  $\delta_{2L} = 0.015$ , an optimum bandwidth length for the longer offset short (STD3) would be 5.4864 mm. For the corresponding center frequency of 6.9 GHz,  $\epsilon_{\text{eff}} = 6.859$ , and  $\lambda = c/f\sqrt{\epsilon_{\text{eff}}}$ , the lengths translate to  $D_{\text{STD}2} = 0.193\lambda$  and  $D_{\text{STD}3} = 0.331\lambda$ .

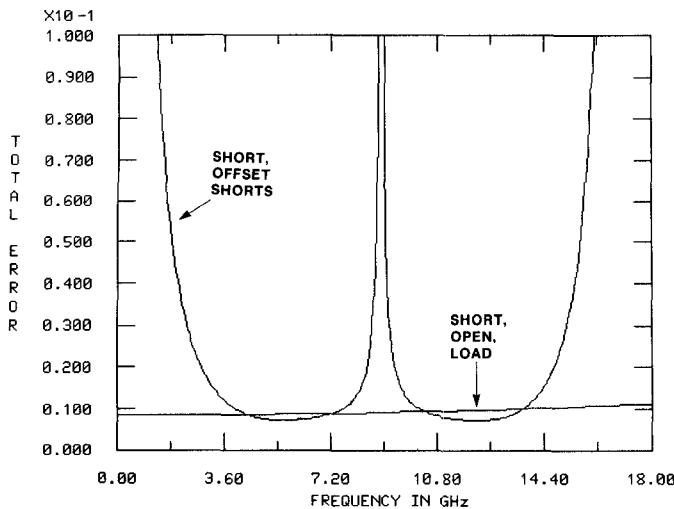


Fig. 2.  $\delta_{\text{TOTAL}}$  versus frequency comparing short, open, load and short offset shorts calibration.  $\delta_{1M} = 0.001$ ,  $\delta_{2L} = 0.005$  for all six standards. DUT is a  $100 \Omega$  resistor. Shorter offset short length =  $D_{\text{STD2}} = 3.2004$  mm; longer offset short length =  $D_{\text{STD3}} = 6.4008$  mm.

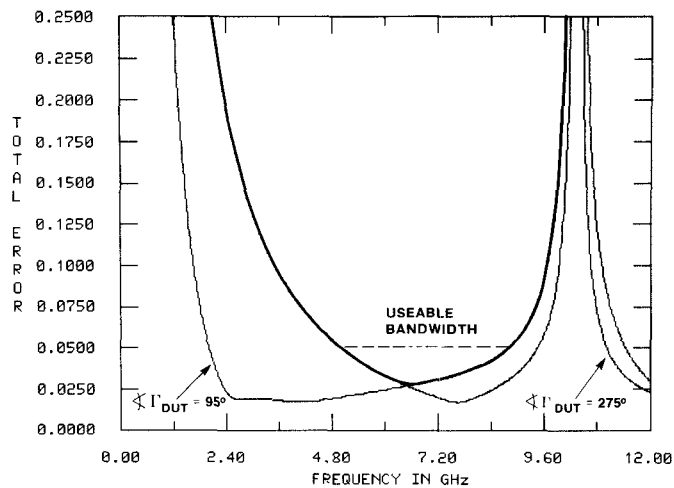


Fig. 3.  $\delta_{\text{TOTAL}}$  versus frequency for different values of  $\Gamma_{\text{DUT}}$ . The usable bandwidth is indicated.  $|\Gamma_{\text{DUT}}| = 0.9$ ,  $\delta_{1M} = 0.001$ ,  $\delta_{2L} = 0.015$ ,  $D_{\text{STD2}} = 3.2004$  mm,  $D_{\text{STD3}} = 5.4864$  mm.

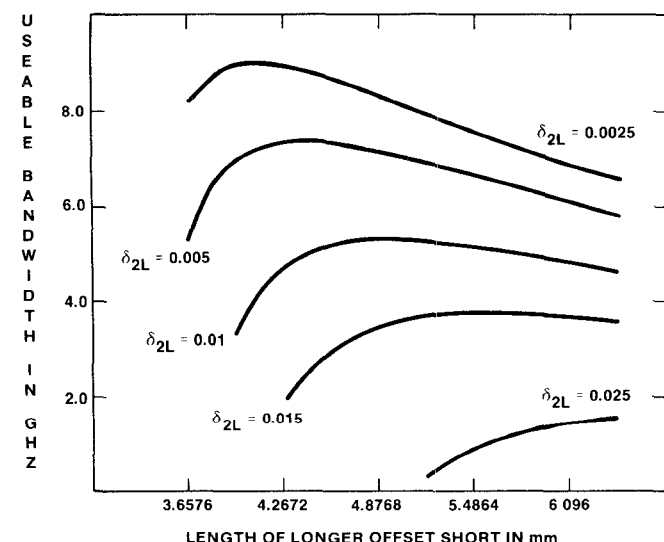


Fig. 4. Usable bandwidth versus length of longer offset short. Length of shorter offset short held constant at 3.2004 mm.

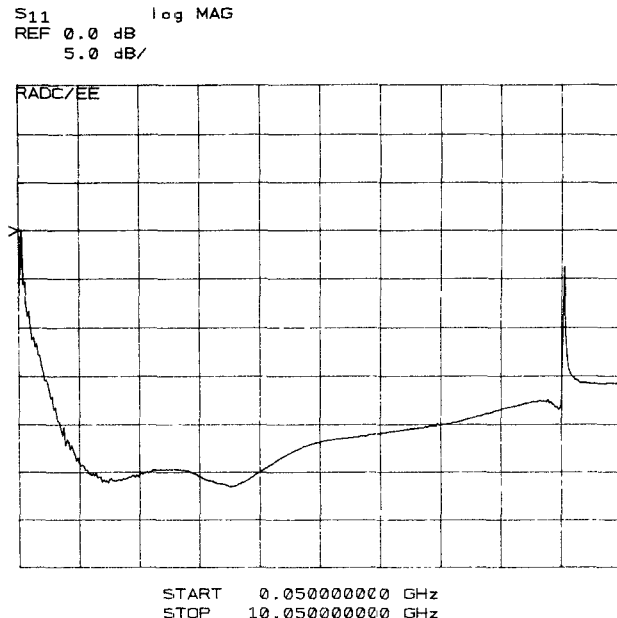


Fig. 5. Experimental results with a  $50 \Omega$  resistor to ground as the DUT. Calibration performed with short, offset shorts standards. Delay of shorter offset short = 27.8 ps. Delay of longer offset short = 54.98 ps

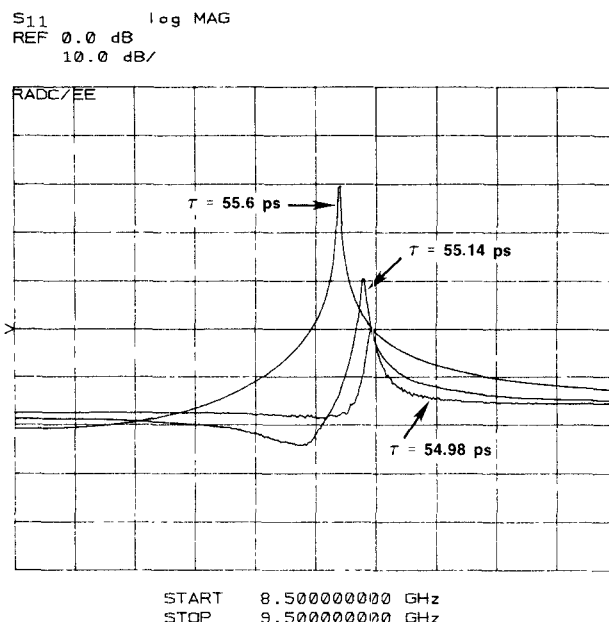


Fig. 6. Experimental spike width with delay,  $\tau$ , of longer offset short as a parameter. Delay of shorter offset short held constant at 27.8 ps.

#### IV. EXPERIMENT

The theory described above can be used with results from simple experiments to obtain precise knowledge of offset short delay and thus optimize measurement accuracy. In addition, an estimate of the remaining uncertainty in the standards may be obtained. This is accomplished using a  $50 \Omega$  load to ground as the DUT since for this case  $|\Gamma_{\text{DUT}}| = \delta_{\text{TOTAL}}$ . Unless a precise estimate of uncertainty is desired, the same quality required of a standard is not needed for this matched load.

Shown in Fig. 5 are measured  $|S_{11}| = |\Gamma|$  data obtained from an HP 8510 after calibration with our microstrip standards (these utilize microstrip connected to edge metallization connected to

the ground plane metallization, with the edge additionally soldered to the fixture end wall). Note the presence of the spikes predicted by theory. The frequency points at which  $|S_{11}| = -10$  dB define a spike width and correspond to  $\delta_{\text{TOTAL}} = 0.316$ . (Other convenient values may be chosen as desired.) Returning to the model,  $\delta_{2L}$  can be varied until the theoretical  $\delta_{\text{TOTAL}} = 0.316$  spike width equals the experimental  $-10$  dB width. Our experimental spike width of 44.7 MHz corresponds to  $\delta_{2L} \approx 0.0039$ , which is an angular uncertainty of  $0.22^\circ$ .

This small value of uncertainty was achieved experimentally as follows. Several measurements of the  $50 \Omega$  DUT were taken using the delay of the longer offset short as a variable parameter. This is illustrated in Fig. 6. The mutually consistent delay which properly characterizes the offset short corresponds to minimum spike width.

## V. SUMMARY AND CONCLUSIONS

The Glasser error analysis theory [6] has been applied to network analyzer accuracy enhancement by offset shorts. The effects of DUT dependence were discussed and a useful calibration bandwidth determined. Data necessary to emulate the HP 8510 were derived and then used in the model to provide realistic results. Convenient techniques for optimizing experimental accuracy and for obtaining an estimate of the uncertainty in actual short, offset short calibration standards were presented. Due to the limited bandwidth properties of offset short calibration, multiple standards are necessary for wideband operation. The importance of the characterization procedures described above continues to apply in the multiple standards case.

The information provided in this paper should contribute to the efficiency of making chip-level measurements in a microstrip environment. This will assist in the design and realization of monolithic microwave integrated circuits. Much of the work is also applicable to offset short calibration in waveguide and other transmission line media.

## ACKNOWLEDGMENT

The authors wish to acknowledge the fixture drawings received from MIT Lincoln Laboratory as well as helpful discussions with W. Piacentini, J. Lambert, C. Berglund, and A. Chu. The inputs of P. Rainville and R. Webster of RADC are also appreciated.

## REFERENCES

- [1] S. Rehnmark, "On the calibration process of automatic network analyzer systems," *IEEE Trans. Microwave Theory Tech.*, vol. MTT-22, pp. 447-458, Apr. 1974.
- [2] R. F. Bauer and P. Penfield, Jr., "De-embedding and unterminating," *IEEE Trans. Microwave Theory Tech.*, vol. MTT-22, pp. 282-288, Mar. 1974.
- [3] D. Ryting, "Analysis of vector measurement accuracy enhancement techniques," presented at Hewlett-Packard RF and Microwave Symp., 1980.
- [4] M. L. Stevens, "Characterization of power MESFETs at 21 GHz," ESD-TR-81-191, M.I.T. Lincoln Laboratory, Lexington, MA, Sept. 1981; AD A106673.
- [5] C. D. Berglund, "Large-signal characterization amplifier design, and performance of K-band GaAs MESFET's," ESD-TR-81-296, M.I.T. Lincoln Laboratory, Lexington, MA, Dec. 1981; AD A110873.
- [6] L. A. Glasser, "An analysis of microwave de-embedding errors," *IEEE Trans. Microwave Theory Tech.*, vol. MTT-26, pp. 379-380, May 1978.
- [7] K. C. Gupta, R. Garg, and R. Chadha, *Computer-Aided Design of Microwave Circuits*, Dedham, MA: Artech House, 1981.
- [8] *HP 8510 Network Analyzer System Operating and Programming Manual*, Hewlett-Packard Company, Santa Rosa, CA, 1985.
- [9] *Introduction to Basic Measurements using the HP 8510*, Hewlett-Packard Company, Santa Rosa, CA, 1984.
- [10] *HP 8510 Network Analyzer Operating and Service Manual*, vol. 1, Hewlett-Packard Company, Santa Rosa, CA, 1984.

- [11] M. Kirschning and R. H. Jansen, "Accurate model for effective dielectric constant of microstrip with validity up to millimetre-wave frequencies," *Electron. Lett.*, vol. 18, pp. 272-273, Mar. 1982.

## On the Scalar Approximation in Fiber Optics

CHING-CHUAN SU, MEMBER, IEEE

**Abstract** — It is widely accepted that the scalar approximation is valid when the gradient of the permittivity distribution  $\nabla\epsilon/\epsilon$  is small enough. Such a condition is rather demanding, however, since it precludes a rapidly varying permittivity distribution, which is usually the case in a practical optical fiber, due to some kind of fluctuation in a fabrication process. In this investigation, we derive the scalar approximation from the electric field integral equation. From the result it is seen that the applicability of the scalar approximation does not depend on the roughness in the permittivity distribution so long as the permittivity in the core is close to that in the cladding.

## I. INTRODUCTION

Mathematics is greatly simplified on applying the scalar approximation to the analysis of the propagation characteristics of guided modes in dielectric waveguides. Early in the development of the dielectric waveguide theory, Gordon [1] and Marcatili [2], among other investigators, applied the scalar approximation (together with other approximations) in studying the inhomogeneous slab waveguide and the rectangular waveguide, respectively. In 1969, in a study mainly on the step-index circular fiber (of which  $\epsilon_r$ , the ratio between the permittivity in the core and that in the cladding, is close to unity), Snyder [3] obtained the scalar characteristic equation from the rigorous vectorial one. In the simplification, those terms which are of order  $\epsilon_r - 1$  or smaller can be discarded. Later, Gloge [4] obtained the same scalar characteristics equation by using a set of field components that are not self-consistent. He noted that the inconsistency in transverse field components is of order  $\epsilon_r - 1$ .

For treating graded-index fibers or, generally, for transversely inhomogeneous fibers, Maxwell's equations in the differential form (Section II) are employed by most researchers. Thereby, it is widely accepted that the scalar approximation is valid when the gradient  $\nabla\epsilon/\epsilon$  is small enough, as noted in [5]–[9], where  $\epsilon$  denotes the relative permittivity distribution in a transverse plane. Suppose the relative permittivity distribution  $\epsilon$  can be expressed as

$$\epsilon(x, y) = \epsilon_1 + (\epsilon_2 - \epsilon_1) P(x, y) \quad (1)$$

where the maximum value of  $P(x, y)$  is unity such that  $\epsilon_2 (> \epsilon_1)$  corresponds to the maximum in  $\epsilon(x, y)$ , and  $P(x, y) = 0$  in the cladding. Having the gradient  $\nabla\epsilon/\epsilon$  small enough requires that the permittivity difference  $\Delta$  be small enough and that the profile  $P(x, y)$  be smooth over the fiber's cross section, where  $\Delta = \epsilon_r - 1$  and  $\epsilon_r = \epsilon_2/\epsilon_1$ . In other words, the scalar approximation could deteriorate if the profile  $P(x, y)$  is rapidly varying (such as at a step discontinuity), even when the permittivity ratio  $\epsilon_r$  becomes close to unity.

A less demanding condition on the scalar approximation can be provided by the formula proposed by Snyder *et al.* [10, eq.

Manuscript received August 18, 1987; revised January 4, 1988.

The author is with the Department of Electrical Engineering, National Tsinghua University, Hsinchu, Taiwan  
IEEE Log Number 8820444.